



Adve

STEM CELLS / Volume 35, Issue 4

Regenerative Medicine |

A Reinterpretation of Cell Transplantation: GFP Transfer From Donor to Host Photoreceptors

Arturo Ortin-Martinez, En Leh Samuel Tsai, Philip E. Nickerson, Miriam Bergeret, Yao Lu, Sheila Smiley, Lacrimioara Comanita, Valerie A. Wallace

First published: 14 December 2016

<https://doi.org/10.1002/stem.2552>

Cited by:8

About Sections



PDF

Tools



Shar

Abstract

The utilization of fluorescent reporter transgenes to discriminate donor versus host cells has been a mainstay of photoreceptor transplantation research, the assumption being that the presence of reporter⁺ cells in outer nuclear layer (ONL) of transplant recipients represents the integration of donor photoreceptors. We previously reported that GFP⁺ cells in the ONL of cone-GFP transplanted retinas exhibited rod-like characteristics, raising the possibility that GFP signal in recipient tissue may not be a consequence of donor cell integration. To investigate the basis for this mismatch, we performed a series of transplantations using multiple transgenic donor and recipient models, and assessed cell identity using nuclear architecture, immunocytochemistry, and DNA prelabeling. Our results indicate that GFP⁺ cells in the ONL fail to exhibit hallmark elements of donor cells including nuclear hetero/euchromatin architecture. Furthermore, GFP signal does not appear to be a consequence of classic donor/host cell fusion or transfecting post-transplantation but is most likely due to material exchange between donor and host photoreceptors. This transfer can be mediated by rods and cones, is bidirectional between donor and host cel



Collectively, these data warrant re-evaluation of the use of image tracing fluorescent reporters in transplantation studies involving the retina and other CNS tissues. Furthermore, the reinterpretation of previous functional rescue data, based on material exchange, rather than cell integration, may offer a novel approach to vision rescue. *STEM CELLS* 2017;35:932–939

Significance Statement

GFP labeled photoreceptors are observed in the outer nuclear layer of recipient retinas following transplantation of GFP-tagged photoreceptors. The historical interpretation of this observation has centered around the migration of donor cells into recipient retina, and maturation of these cells into functional photoreceptors. This study challenges this interpretation by showing that there is almost no donor cell integration into intact retinal tissue, and provides evidence that the origin of the GFP signal in the recipient retina is due to exchange of GFP signal between donor and host retinal cells. This work reveals that the adult retina is not as receptive to donor cell integration as was previously thought and deepens our understanding of how photoreceptor therapy, via material exchange, could work therapeutically.

Introduction

Transplantation of photoreceptors is reported to partially rescue vision in blind animal models 1-5, an effect that has been attributed to the physical integration of donor photoreceptors. Reporter transgenes have garnered in this interpretation, as the extent of rescue correlates with the number of GFP⁺ cells in the outer nuclear layer (ONL) of host retinas 1-5. We described the utility of cone and cone/rod hybrid precursor cell (termed “cods”) transplantation through generation of *Ccdc136*^{GFP/+} gene trap, and *Nrl*^{-/-}; *Ccdc136*^{GFP/+} compound mutant mice, respectively 6. Although we observed GFP⁺ photoreceptors in the recipient ONL following transplant, we reported an unexpected mismatch in nuclear morphology between donor and integrated cells 6. Here, we examined the relationship between GFP⁺ cells the ONL of transplant recipients and donor cell identity. Rather than



Materials and Methods

Animals and Genotyping

All experiments were approved by the University Health Network Research Ethics Board and adhered to the guidelines of the Canadian Council on Animal Care. Animal husbandry was in accordance with the Association for Research in Vision and Ophthalmology (ARVO) Statement for the Use of Animals in Ophthalmic and Vision Research. Animals were maintained under standard laboratory conditions and all procedures were performed in conformity with the University Health Network Animal Care Committee (protocol 3499.10). Mouse strains are summarized in Supporting Information Table S1. *C57BL/6J* mice (Charles River), *Crx*^{-/-} **7**, and *Nrl*^{-/-} **8** of both sexes were used as transplantation recipients, all of them being 6–14 weeks the time of transplantation. *Nrl-GFP* **9**, *Ccdc136*^{GFP/+}, and *Nrl*^{-/-};*Ccdc136*^{GFP/+} **6** and *ROSA*^{mT/mG} mice were used as photoreceptor donors at postnatal P3–P5. For homozygous lines, genotyping was performed by extracting genomic DNA from ear clip samples through incubation in 200 μ l alkaline lysis buffer (25 mM NaOH, 0.2 mM EDTA pH 8.0) for 1 hour at 95°C. Samples were neutralized with 200 μ l neutralization buffer (40 mM Tris-HCl) and genotyped by the polymerase chain reaction (PCR) using primer sets indicated in Supporting Information Table S2.

Donor Cell Preparation, Labeling, and Fluorescence-Activated Cell Sorting

To prepare donor cells for transplantation, retinas from *Ccdc136*^{GFP/+}, *Nrl*^{-/-};*Ccdc136*^{GFP/+}, and *Nrl-GFP* mice were harvested in CO₂ independent media (Fisher Scientific) and dissociated with papain (Worthington Biochemical, Lakewood, New Jersey, www.worthington-biochem.com) according to the manufacturer's directions. Cells were washed in Ca²⁺/Mg²⁺ free phosphate buffered saline (PBS) and counted using 0.4% Trypan blue (Thermo Fisher, Mississauga, Canada, www.thermofisher.com) as a viability counter stain before being re-suspended in 5% BSA 2 mM EDTA 25 mM HEPES 0.005% DNase in Ca²⁺/Mg²⁺ free PBS, and passed through a strainer (40 μ m) into FACS tubes (BD Falcon). Cells were then sorted for GFP fluorescence using an Aria III (BD Biosciences, Mississauga, Canada, www.BD.com/ca) equipped with a 488-nm laser and collected in 10% BSA in Ca²⁺/Mg²⁺ free PBS. The sort was performed using an 85 μ m nozzle at 45 psi, and a flow rate that allowed collecting at 5000 events per second. The data acquisition, analysis, and image preparation were carried out using the instrument software FACSDiva (BD Biosciences). The GFP gating histograms are shown in Supporting Information Figure S1A. Sorted GFP⁺ and unsorted cells were resuspended at a concentration of 200,000



intraocular injections separated by 4 hours (summarized in Supporting Information Fig. S1B) with 5-ethynyl-2'-deoxyuridine (50 mg/kg, 5 mg/ml stock concentration, Life Technologies EdU, Burlington, Canada, www.lifetechnologies.com). The retinas were dissociated at P4 and GFP⁺ photoreceptors were enriched by FACS. EdU labeling in the GFP⁺ donor cell population was confirmed at ≥40% EdU coverage of postmitotic donor cells (Supporting Information Fig. S1C). EdU detection was performed using an Alexa Fluor 647 Click-iT (azides/alkyne) reactor as per manufacturer's instructions.

Subretinal Injections

Adult recipient *C57BL/6J*, *Nrl-GFP*, *Crx^{-/-}*, and *Nrl^{-/-}* mice (6–8 weeks old) were anesthetized using a mixture of ketamine (100 mg/ml, Vetalar) at 50mg/kg and medetomidine (1 mg/ml, Dexdomitor, Zoetis, Kirkland, Canada, www.zoetis.ca) at 1mg/kg in sterile 0.9% NaCl administered intraperitoneally. Eyes were dilated using 1% tropicamide (Mydriacyl, Alcon, Mississauga, Canada, www.alcon.ca) drops, followed by application of a 0.2% hydromellose (Genteal, Novartis, Mississauga, Canada, www.novartis.ca) to maintain proper lubrication of the eyes. All injections were performed in the left eye. The eye was gently prolapsed and the animal immobilized using a latex dam customized to allow free blood circulation. Injections were performed using a nanoinjector (Harvard Apparatus, Saint Laurent, Canada, www.harvardapparatus.com) and two surgical microscopes. The retina was visualized for confirmation of cell deposit using a glass coverslip under a dissection microscope. A fluorescence microscopy-guided microinjection was performed by a second surgeon located orthogonal to the viewing microscope. A scleral incision was made in the dorsal side, posterior to the limbus using a 30-gauge needle. Next, a blunt 32-gauge needle (Hamilton, Montreal, Canada, www.coleparmer.ca) was inserted tangentially into the subretinal space (SRS) and advanced into the SRS under the guidance of the person visualizing the fundus. Once the needle was located in the SRS, a small incision was made in the cornea to relieve the intraocular pressure. 1.0 μl cell suspension (dose varying between 50,000 and 200,000 donor cells) was injected over 30 seconds, followed by a 60-second pause to allow for equilibration of pressure and to prevent efflux. The needle was then slowly retracted and the animal anesthesia reversed using an intraperitoneal injection of 1 mg/kg atipamezole (5 mg/ml Revertor, Zoetis). Animals were kept on a heating pad until fully recovered.

Tissue Processing, Histology, and Immunocytochemistry

Mice were harvested 21 days postsurgery by exsanguination with PBS (0.14 M NaCl, 2.5 mM KCl, 0.2 M Na₂HPO₄, 0.2 M KH₂PO₄) and transcardially perfused with 4% paraformaldehyde (PFA). Eyes were then marked with a silver nitrate stick on the dorsal part of the cornea.



equilibrated in 30.50 30% sucrose in PBS. OCT (tissue-tek) for 1 hour and subsequently oriented and embedded in plastic molds. Tissue blocks were stored in -80°C . Tissue was sectioned at $20\ \mu\text{m}$ thickness onto Superfrost Plus slides (Fisher Scientific) on a Leica cryostat and air-dried for 1 hour before being stored in a slide box with desiccant at -20°C . For immunocytochemistry the sections were screened and selected to exclude the injection site. Sections were blocked with 10% donkey serum (DS) (Sigma Aldrich, Oakville, Canada, www.sigmaaldrich.com) 0.3% Triton-X in PBS for 1 hour at room temperature. Primary antibodies (Supporting Information Table S3) were diluted in 5% DS 0.15% Triton-X in PBS for overnight staining of retina sections at 4°C . After three washes with PBS, sections were incubated with fluorescent secondary antibody diluted in 5% DS 0.15% Triton-X in PBS for 1 hour at room temperature in a light protected humidified box. Nuclei were counterstained with fluorescent DNA-binding dye, Hoechst 33342 (Life Technologies). Slides were washed and glass coverslips were mounted with DAKO mounting media.

Confocal Imaging, Cell Counting, and Statistics

Wide-field fluorescent images were acquired using an Axioimager M1 (Carl Zeiss Inc., www.zeiss.com). 2048×2048 resolution confocal images were acquired using a LSM 780 (Carl Zeiss Inc.) with 2% laser intensities and no greater than 800 gain, with a minimum of 4x averaging. Objectives (20x, 40x water immersion, 63x oil immersion) and a 1.0 Airy Unit pinhole determined voxel depth on z-stacks. Image acquisition parameters were maintained for all comparative images. Images were processed using Photoshop CS4 or CS6 and any adjustments were made to the entire image and equally for all comparative images. The number of GFP⁺ cells in the ONL was quantified by counting all cells with the entire cell body located in the host ONL. The total number of GFP⁺ cells per eye was determined by extrapolation, based on quantification of every 4th section. Nuclear mismatching and colocalization values were generated from counts in alternate sections that were visualized with 40x and 63x objectives. Orthogonal images were generated using Zeiss Zen software. Animals devoid of any bolus cells in the SRS were excluded from the analysis. All data are presented as mean \pm SEM.

Results and Discussion

Mismatch Between GFP⁺ Donor and Recipient Cells

To investigate the identity of GFP⁺ cells located the ONL (ONL-GFP) of photoreceptor transplant recipients, we exploited the distinct nuclear architecture of rods and cones in vivo (10, Supporting Information Fig. S2A). Consistent with previous reports 1, 3, ONL-GFP cells in



GFP⁺ cell with cone-like morphological and cytochemical features (Fig. 1D), suggesting a fate mismatch between donor rods and ONL-GFP cells in recipients. To investigate whether this donor/host mismatch extends to cones, we transplanted P3–P5 *Nrl*^{-/-}; *Ccdc136*^{GFP/+} cods (co-GFP) or *Ccdc136*^{GFP/+} cones (cone-GFP) into rod-dominant wildtype recipients. Cod and cone cells in the SRS exhibited cone-like nuclei and marker expression (Fig. 1C, 1D, Supporting Information Fig. S2B–S2B’), whereas >99% ONL-GFP cells were rod-like and negative for cone markers (Fig. 1C, 1D, 1F). Similarly, in rod-GFP transplanted cod-only *Nrl*^{-/-} retinas, ~80% of ONL-GFP cells had a cone nuclear morphology (Fig. 1E, 1F), and all coexpressed Cone arrestin (CAr), a cone marker (Fig. 1E), indicating that rod transplantation generates a cod identity in *Nrl*^{-/-} recipients. The extent of mismatch was not a function of the number of GFP⁺ cells in the recipient ONL, although notably, these cells were abundant in *Nrl*^{-/-} recipients (Fig. 1G), which is consistent with previous reports [2](#). In contrast, transplantation of cod-GFP and cone-GFP cells into *Crx*^{-/-} mice, a mouse model of photoreceptor degeneration [7](#), appeared consistent with *bona fide* cell integration (Supporting Information Fig. S3), as evidenced by GFP/CAr colocalization and donor-matched nuclear architecture in ONL-GFP cells. These data provide evidence that GFP labeling observed in recipient retinas following photoreceptor transplantation favors the most abundant cell type present in recipient retinas, with the exception of that observed in the degenerating retina.

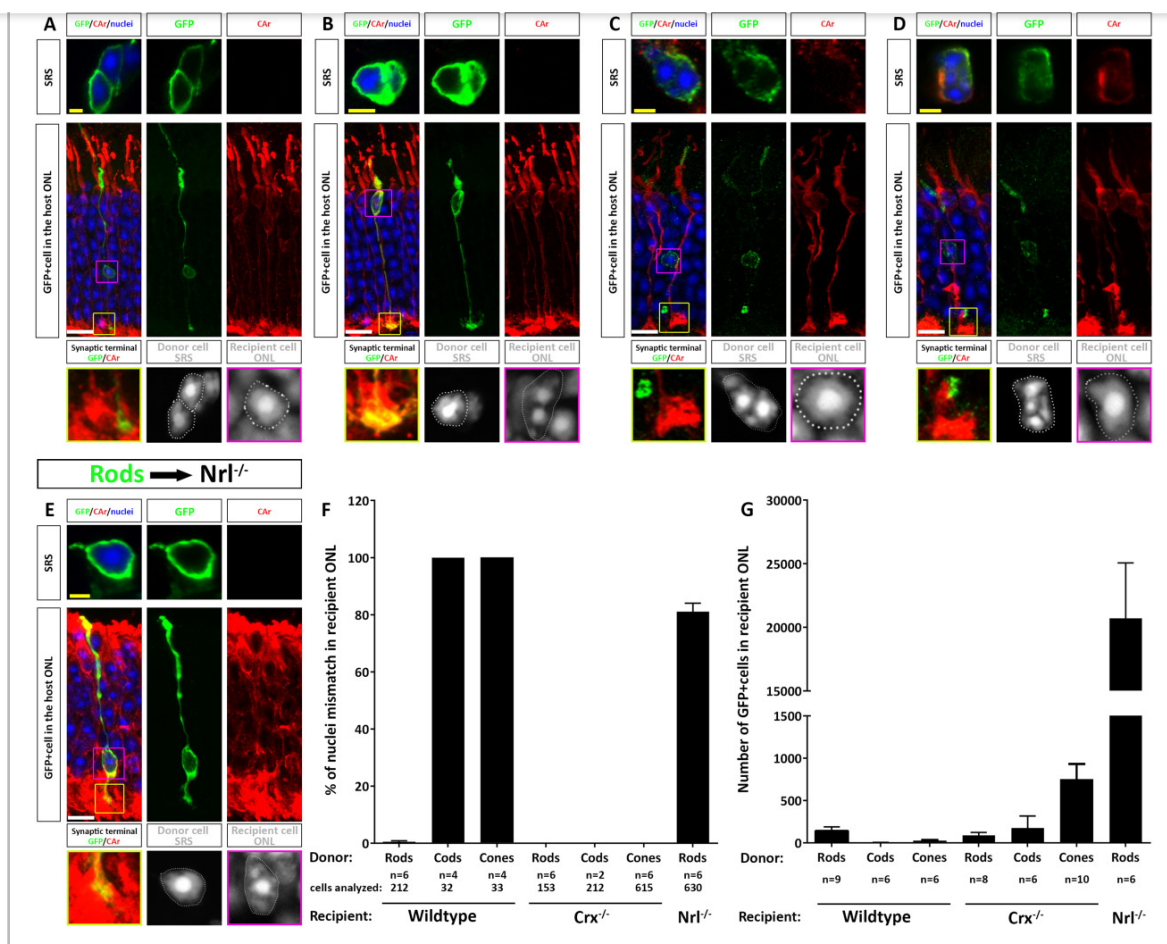


Figure 1

[Open in figure viewer](#) | [PowerPoint](#)

GFP-labeled cells in the outer nuclear layer (ONL) of photoreceptor transplant recipients exhibit nuclear and morphological mismatch to donor cells. All mice were sacrificed at 21 days post-transplant. **(A-E)**: Immunohistochemistry for GFP, Cone arrestin (CaR) and nuclei in retinal sections of wildtype recipients transplanted with rod-GFP (A, B), cod-GFP (C), cone-GFP cells (D) and *Nrl*^{-/-} recipients transplanted with rod-GFP cells (E). (A, C, D) Irrespective of the donor cell nuclear morphology in the subretinal space (SRS), GFP⁺ cells in the recipient ONL have a rod identity based on nuclear morphology (bottom right panel) and the presence of GFP⁺ spherules (bottom left panels). The only exception is (B) where in a rod-GFP transplanted wildtype retina we observed a single GFP⁺ in the ONL with a cone nuclear morphology (lower right panel), a cone pedicle (recipient cell left panel) and colocalization with CaR (middle panels). (E) A cod-like nuclear morphology (lower right panel) and cod pedicle (lower left panel) is observed in the ONL of the *Nrl*^{-/-} recipients when donor cells were



switch, or previously uncharacterized transfer. Fusion of GFP-labeled hematopoietic cells results in binucleated cerebellar neurons 11, 12. Orthogonal-examination of ONL-GFP cells in all recipients failed to identify a binucleate event (not shown). Rod photoreceptors originate from the S-cone lineage 13, raising the possibility that a fate switch from rod to cone could account for the GFP labeling in cones in rod transplanted retinas. To address this possibility, we transplanted P4 rod-GFP cells that were pre-labeled in vivo with the thymidine-analogue EdU (Supporting Information Fig. S1B, S1C), into $Nr1^{-/-}$ recipients. This labeling paradigm serves as an indelible lineage-independent DNA marker, which should be detectable if donor cells switch fate after integrating into the recipient retina. We utilized $Nr1^{-/-}$ recipients, which exhibit high rates of ONL-GFP cells post-transplantation (Fig. 1F), to maximally identify EdU⁺ cells in the recipient ONL. Although we detected EdU⁺/GFP⁺ cells in the SRS, we did not detect a single EdU⁺ nucleus in the ONL (>7800 ONL-GFP cells examined—Fig. 2A-2C) arguing strongly against donor cell integration as the source of ONL-GFP cells. Fusion or transfer has not been reported in experiments where rod-GFP cells were transplanted into cytoplasmic cyan fluorescent reporter recipients 1. Utilizing a different approach, we transplanted retinal dissociates from P3 to P5 mice expressing membrane-tethered tdTomato ($ROSA^{mT/mG}$, Supporting Information Fig. S4A-S4E”) into rod-GFP recipients (Fig. 2D, 2E). We identified tdTomato/GFP colabeled cells in the ONL, demonstrating transfer of a membrane-tethered reporter (Fig. 2D, Supporting Information Fig. S4A-S4E”). Furthermore, we observed transfer of GFP (Fig. 2E) and CAR (Supporting Information Fig. S4F-S4G”), but not S-Opsin (Supporting Information Fig. S2C), which are expressed in the recipient retinas, to the donor cells in the SRS, suggesting that hetero-donor cell transfer is also possible for some proteins.

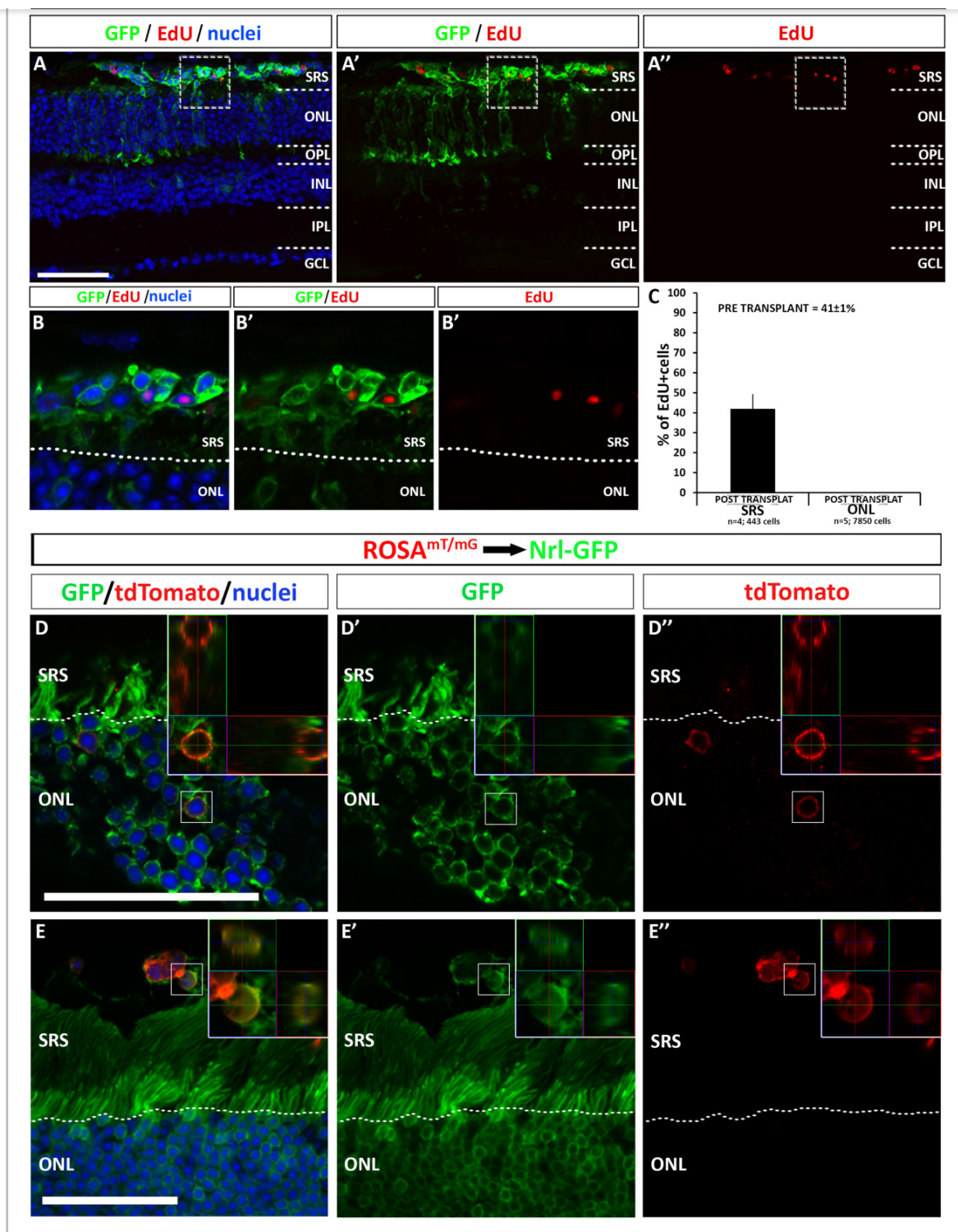


Figure 2

[Open in figure viewer](#) | [PowerPoint](#)

Membrane-tethered tdTomato transfers from donor to host photoreceptors, while donor nuclei fail to migrate into recipient retinas. **(A)**: Maximum intensity



elements are required for donor/host exchange. Surprisingly, 452/459 in vivo columns of ONL-GFP cells in *Nrl*^{-/-} recipients were associated with brightly GFP-labeled, donor cells located at the outer limiting membrane (OLM) (Fig. 3A). We also observed what appears to be physical contact between donor/host cells in transplanted retinas (Fig. 3B). Previously, disruption of the OLM was associated with increased numbers of ONL-GFP cells in recipients 14, 15. Staining for the OLM marker Zo1 in control and *Nrl*^{-/-} retinas revealed mislocalization at points of putative GFP transfer (Fig. 3C, 3D), suggesting that OLM breaks could facilitate cell-cell contact or GFP transfer via noncontact-mediated mechanisms. Comparison of uninjected, sham-injected, *Nrl*^{-/-}, and *Crx*^{-/-} recipients (Supporting Information Fig. S6) identified variability in OLM integrity across all transplant contexts, suggesting that graded OLM disruptions may be variably permissive to GFP transfer.

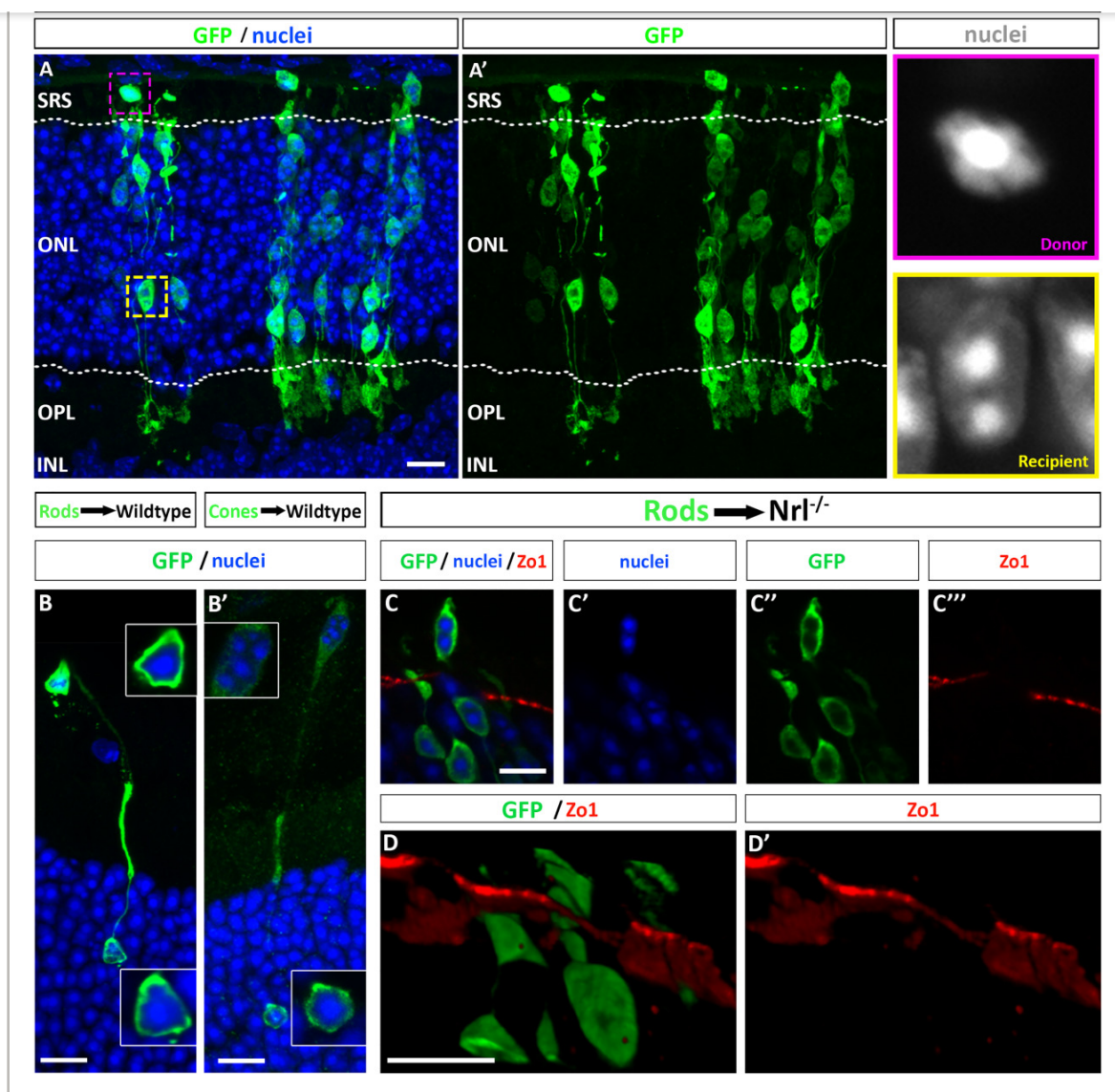


Figure 3

[Open in figure viewer](#) | [PowerPoint](#)

Enhanced GFP transfer observed when donor and recipient cells are in close contact and in the proximity of disrupted OLM. **(A)**: Donor cells located directly above columns of GFP⁺ cells in the ONL of *Nrl*^{-/-} retinas transplanted with rod-GFP cells. **(B)**: Examples of contact between donor photoreceptors in the subretinal space (SRS) and GFP⁺ cells in the host ONL. **(C)**: GFP⁺ cells localize in the SRS and ONL to sites of OLM disruption, marked by gaps in Zo1 staining. **(D)**: Off angle 3D rendering of OLM breaches, through which GFP⁺ cells reside. Abbreviations: GFP, green fluorescent protein; INL, inner nuclear layer; IPL, inner plexiform layer; ONL, outer nuclear layer; OPL, outer plexiform layer; SRS, subretinal space. Scale bar: 10 μm



in INL cells, which would represent second-order transfer. Screening revealed low-level sign in INL cells (Fig. 4A), situated below areas of high ONL-GFP expression in rod-GFP to *Nrl*^{-/-} transplants. Coimmunolabeling for *Vsx2*/GFP (Fig. 4C, Supporting Information Fig. S5A) and glutamine synthetase/GFP (Fig. 4E, Supporting Information Fig. S5B) identified GFP signal in bipolars and Müllers, respectively, whereas Calbindin-D28k (Fig. 4D) failed to detect GFP in horizontal cells. Imaging of Rod-GFP donor retinas using the same imaging parameters identified similar GFP signal the INL, but not in wildtype and control regions (Supporting Information Fig. S5D-S5E). GFP/Iba1 staining failed to identify GFP in phagocytic microglia (Supporting Information Fig. S5C).

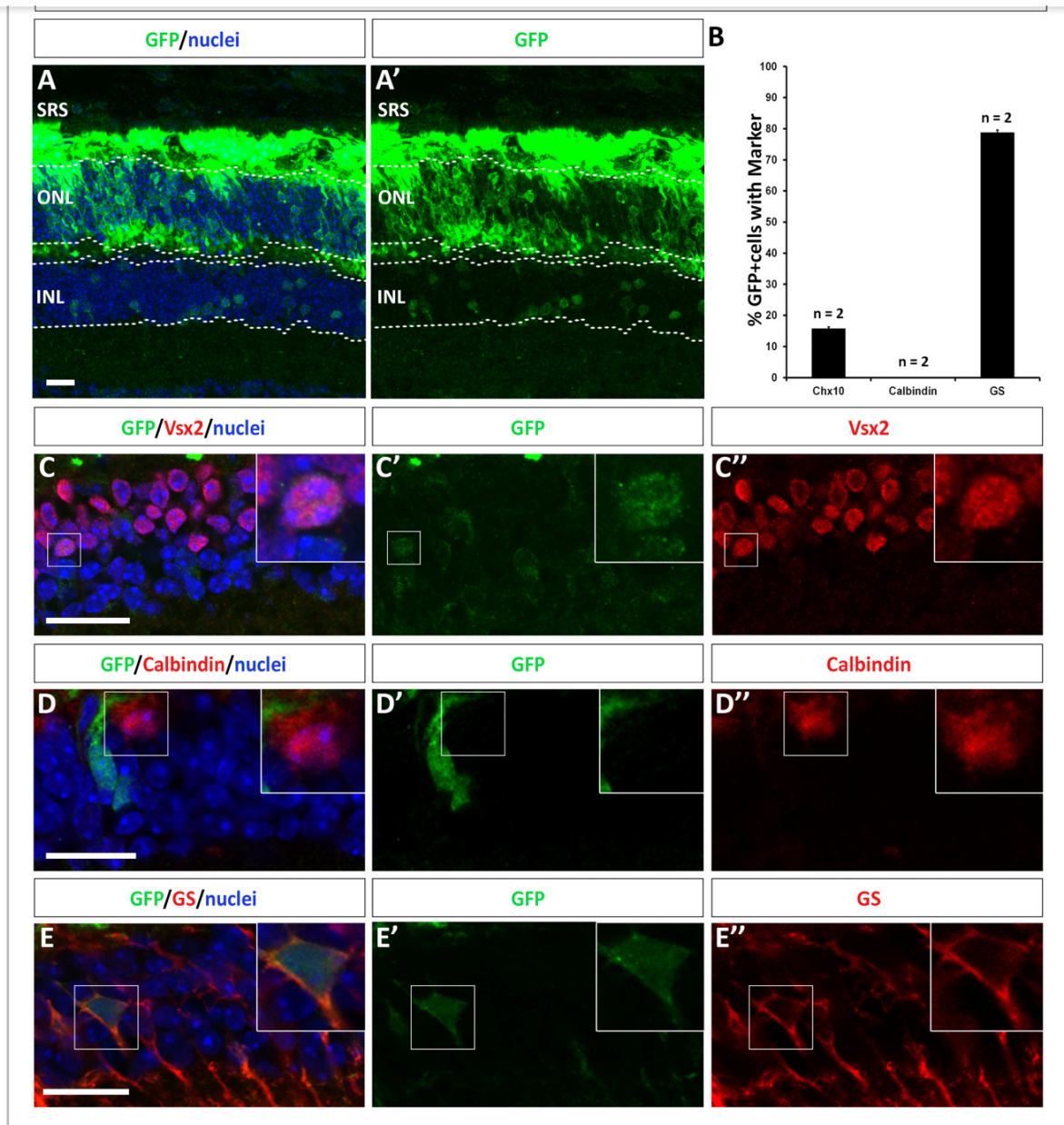


Figure 4

[Open in figure viewer](#) | [PowerPoint](#)

GFP transfer is observed in the inner nuclear layer of recipient retinas. **(A)**: Presence of GFP in the INL of an *Nr1*^{-/-} recipient following transplant with rod-GFP cells. **(B)**: Histogram showing the proportion of GFP⁺ cell subtypes in the INL. **(C)**: A subset of GFP labeled cells in the INL are colabeled with Vsx2. **(D)**: No colabeling of GFP and Calbindin was observed. **(E)**: Majority of GFP⁺ cells in the INL colabel with glutamine synthetase. Abbreviations: GFP, green fluorescent protein; GS, glutamine synthetase; INL, inner nuclear layer; IPL, inner plexiform layer; SRS, subretinal space; ONL, outer nuclear layer; OPL, outer plexiform layer.



retinas transplanted with GFP+ cone and rod photoreceptors, an interpretation that is in agreement with recent findings from other research groups [16](#), [17](#). Transfer requires intact photoreceptors, is associated with cell contact and OLM disruption, and is bidirectional (summarized in Supporting Information Fig. S7). The putative transfer of cone proteins from host to donor photoreceptors suggests that the exchange of other functionally important photoreceptor proteins is likely, which could explain vision rescue reported in blind mice transplanted with photoreceptors [1](#), [2](#). Consequently, data pertaining to donor/recipient age OLM disruption [14](#), and marker-based stratification [18](#) describe the conditions for GFP transfer rather than cell integration per se. Donor/host DNA and mitochondrial transfer [19](#), [20](#), and intercellular exchange via microvesicle/exovesicle GFP [21](#), [22](#), tunneling nanotubes [23](#) have been described in various systems, offering prospective cellular transfer mechanisms. While intercellular transfer of material raises safety concerns for cell-based therapies in the eye and beyond, it also has the potential to be exploited for therapeutic applications.

Acknowledgments

We thank Drs. van der Kooy, Bremner, Monnier, and Schuurmans for helpful discussion and Drs. van der Kooy and Hui for sharing reagents. E. L.S. Tsai and M. Bergeret are recipients of Vision Science Research Program studentships and A. Ortin-Martinez is a recipient of a postdoctoral fellowship from the McEwen Center for Regenerative Medicine. This work was supported by operating grants to V. A. Wallace from Brain Canada, Foundation Fighting Blindness, Ontario Institute of Regenerative Medicine and Krembil Foundation.

Author Contributions

A.O.M.: Concept and design, collection and assembly of data, Data analysis and interpretation
E.L.S.T.: Concept and design, collection and assembly of data, Data analysis and interpretation
P.E.N.: Concept and design, collection and assembly of data, data analysis and interpretation
manuscript writing; Y.L.: collection and assembly of data; M.B.: Collection and assembly of data, data analysis and interpretation; S.S.: Collection and assembly of data, data analysis and interpretation; L.C.: Concept and design, collection and assembly of data, data analysis and interpretation; V.A.W.: Concept and design, financial support, data analysis and interpretation manuscript writing.

Potential Conflict of Interest and Financial Disclosure

No competing interests declared.



References



Citing Literature



© 2018 AlphaMed Press
STEM CELLS
STEM CELLS Translational Medicine
The Oncologist



AlphaMed Press | 318 Blackwell Street | Durham | NC | [Contact Us](#)

[About Wiley Online Library](#)

[Help & Support](#)

[Opportunities](#)

[Connect with Wiley](#)

Copyright © 1999-2018 John Wiley & Sons, Inc. All rights reserved



